Supplementary Figure 1. Related to Figures 1 and 2.

a

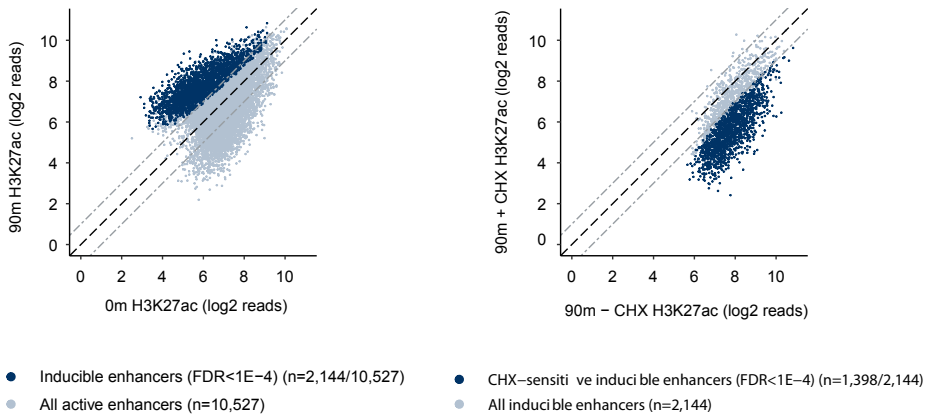

b

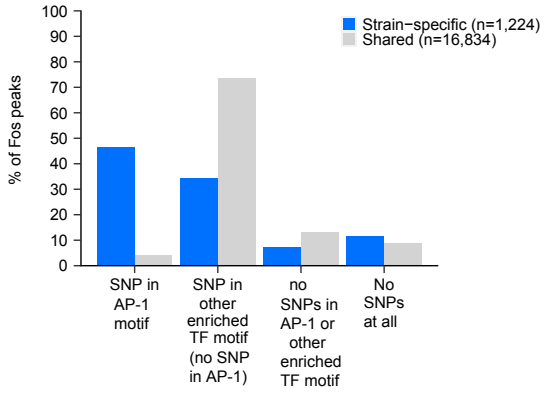

Supplementary Figure 2. Related to Figure 3.

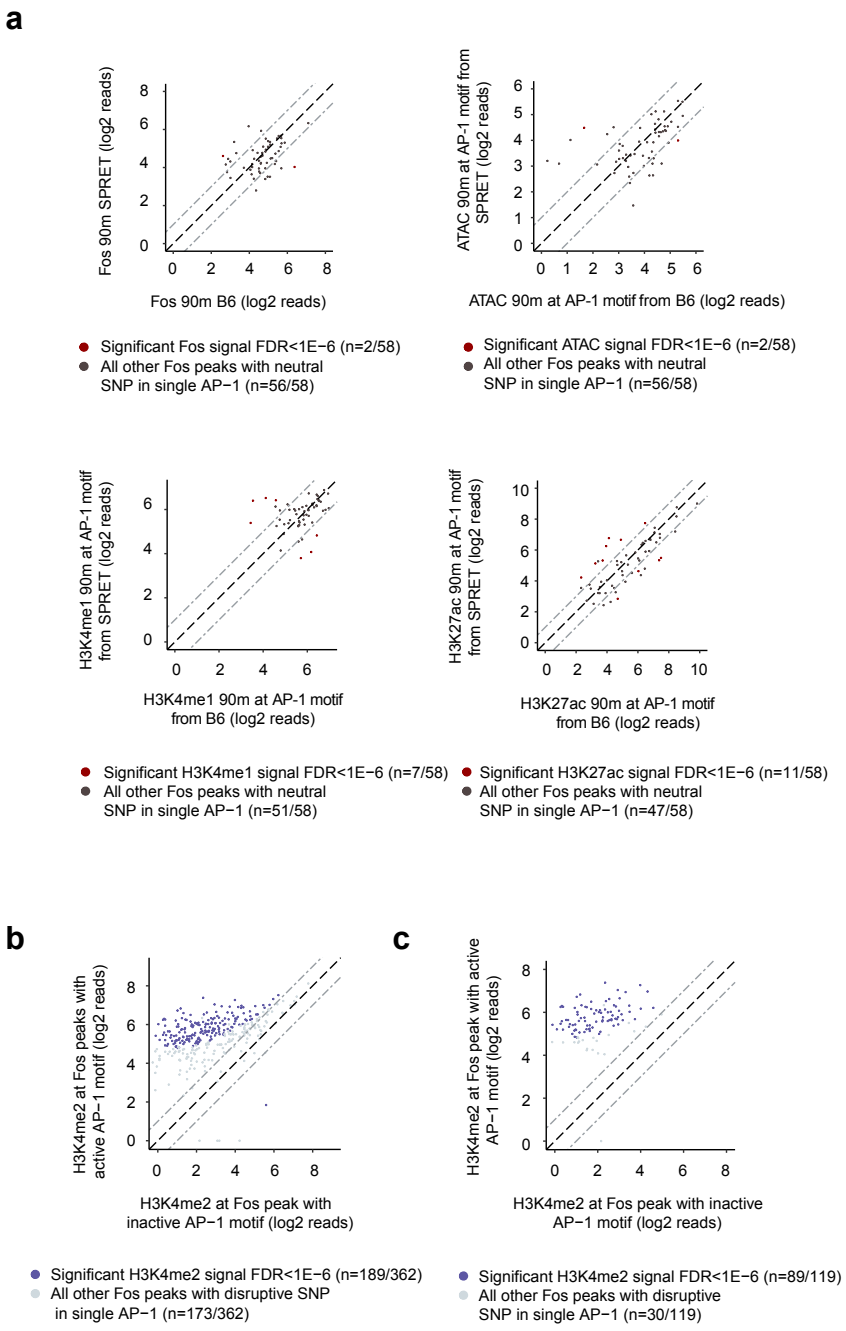

Supplementary Figure 3. Related to Figure 6.

a

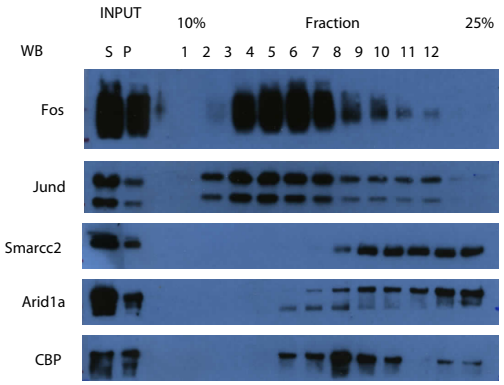

Supplementary Figure 4. Related to Figure 7.

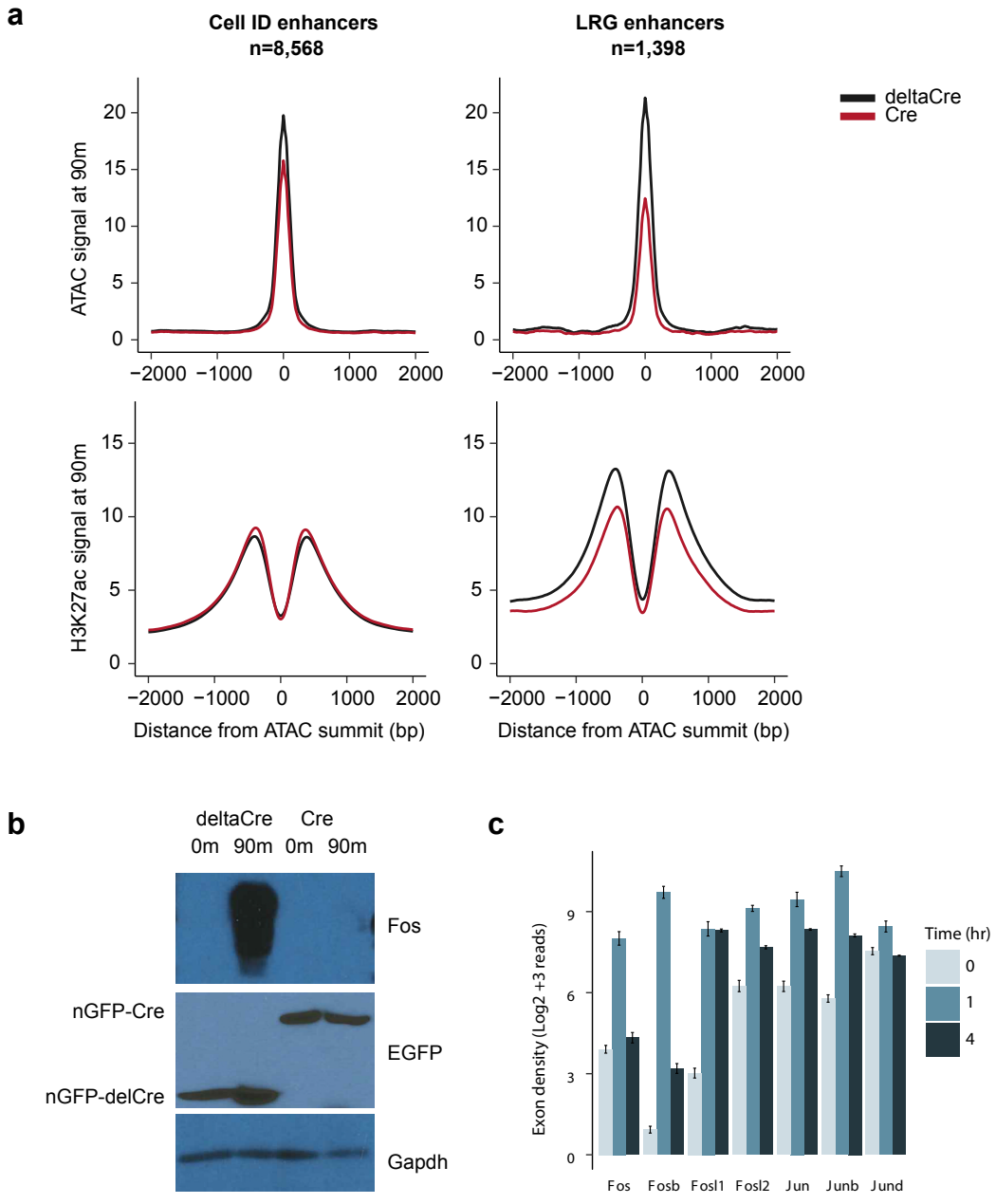

Supplementary Figure 5. Related to Figure 7.

a

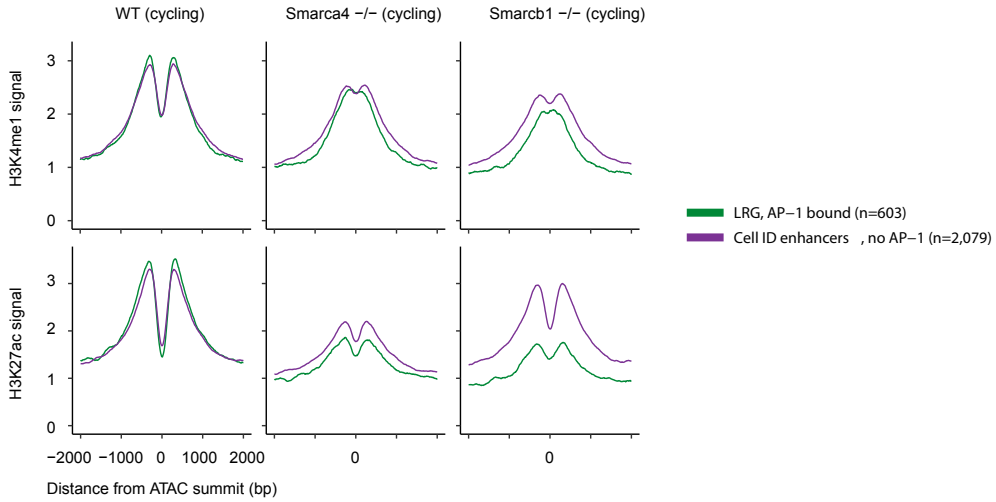

Supplementary Figure 6. Related to Figures 1-7.
Models of signal-dependent enhancer selection by AP-1 TFs and SWI/SNF

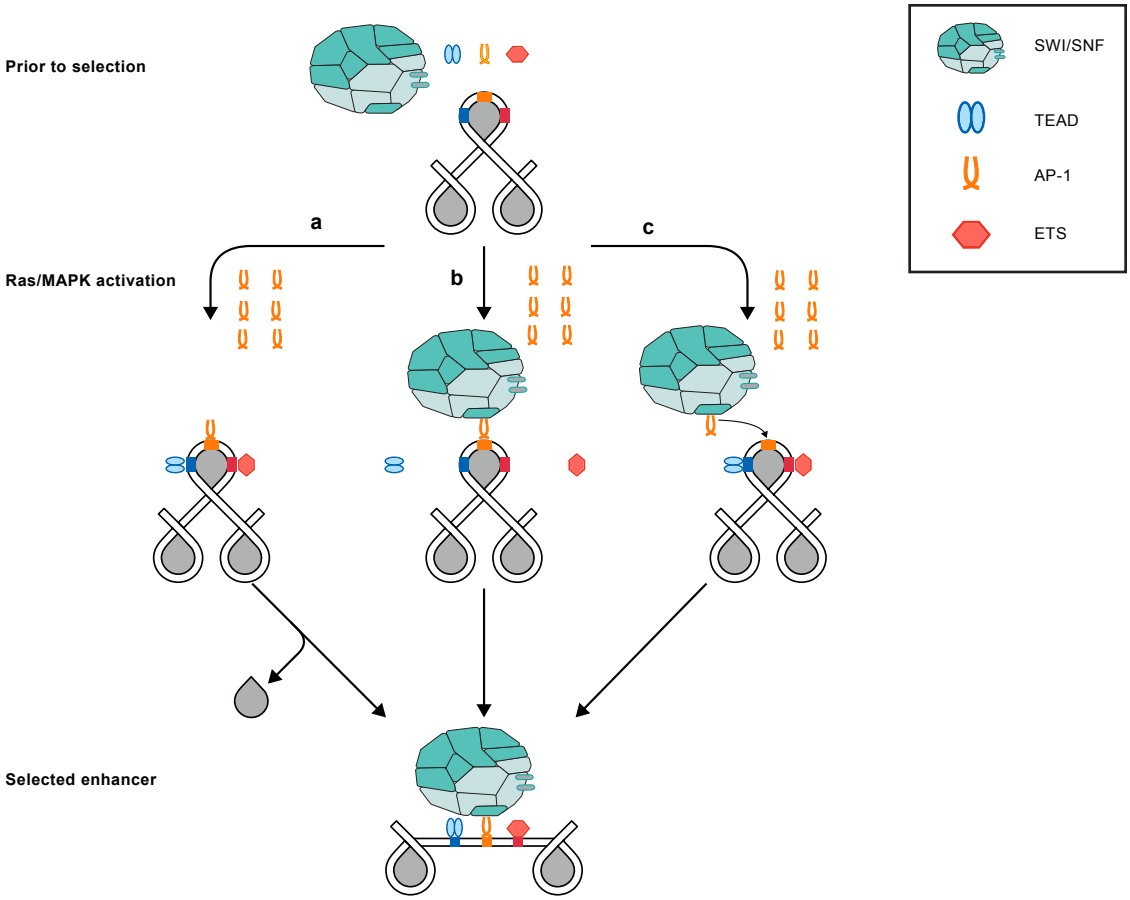

Supplementary Figure Legends

Supplementary Figure 1. Related to Figures 1 and 2:

a) (Left panel) H3K27ac ChIP-seq signal at all H3K27ac peaks distal to gene TSSs that overlap with an ATAC-seq peak identified in either condition (0m, 90m serum stimulation) and have significantly higher H3K4me1 signal than H3K4me3 (n=10,527). Enhancers with a significant increase in H3K27ac signal at 90m (n=2,144) are indicated in dark blue. Dashed gray lines indicate a 2-fold change. (Right panel) Effect of cycloheximide (CHX) treatment on enhancers that exhibit a significant increase in H3K27ac upon serum stimulation (from **a**). Enhancers with a significant decrease in H3K27ac signal at 90m with cycloheximide treatment (n=1,398) are indicated in dark blue. Dashed gray lines indicate a 2-fold change. **b**) Percentages of strain-specific or shared Fos peaks with SNPs in the indicated subsets of these two groups.

Supplementary Figure 2. Related to Figure 3:

a) Scatter plots of Fos ChIP-seq signal or enhancer associated chromatin features for the subset of Fos-bound selected enhancers that contain a single AP-1 motif with a mutation that is not predicted to disrupt AP-1 binding (n=58; also plotted as orange triangles in **Figure 3a**). Highlighted points indicate enhancers at which the signal of the indicated chromatin feature was significantly strain-specific (FDR<10^{-6}). **b**) Scatter plot of H3K4me2 ChIP-seq signal for the subset of the enhancers with significant strain-specific Fos binding in **Figure 3b** that no longer have a Fos peak detected in the strain in which the AP-1 motif is mutated (n=362/434). H3K4me2 ChIP-seq was performed from C57Bl/6JXSPRET/EiJ F1 hybrid MEFs. Highlighted points indicate enhancers at which H3K4me2 was significantly allele-specific (FDR<10^{-6}). **c**) Scatter plot of H3K4me2 ChIP-seq signal from each allele for the strain-specific selected subset of the enhancers in **b**) (n=119; also plotted as

orange triangles in **Figure 3f**). Highlighted points indicate enhancers at which H3K4me2 was significantly allele-specific (FDR<10^{-6}).

Supplementary Figure 3. Related to Figure 6:

Western blots for indicated proteins from 10-30% glycerol gradient centrifugation fractions (1-12 out of 15) of nuclear extracts from MEFs stimulated with serum for 90m. The fractions contain protein complexes increasing in size from fraction 1 (10% glycerol) to 12 (~25% glycerol). For inputs, S=soluble fraction loaded onto gradient, P=insoluble pellet.

Supplementary Figure 4. Related to Figure 7:

a) Aggregate plots of ATAC-seq (top row) and H3K27ac ChIP-seq (bottom row) signal at different classes of enhancers in *Fos*$^{fl/fl}$;*Fosb*$^{fl/fl}$;*Junb*$^{fl/fl}$ MEFs infected with either Cre-EGFP lentivirus or recombinase deficient Cre-EGFP lentivirus (delta-Cre). **b**) Western blots of protein lysates from nGFP-Cre and nGFP-delta-Cre infected *Fos*$^{fl/fl}$;*Fosb*$^{fl/fl}$;*Junb*$^{fl/fl}$ MEFs. **c**) Expression of AP-1 family TFs (exon density from ERCC spike-in normalized mRNA-seq) at 0, 1, or 4 hours after serum stimulation. Error bars indicate standard error from 3 biological replicates.

Supplementary Figure 5. Related to Figure 7:

Aggregate plots of H3K4me1 and H3K27ac ChIP-seq signal at different classes of enhancers in WT, *Smarca4* $^{-/-}$, or *Smarcb1* $^{-/-}$ MEFs cultured continuously in 10% serum (Alver et al., 2017). For each condition, Cre recombinase and a puromycin resistance gene were introduced by retroviral infection to remove floxed alleles from *Smarca4*$^{fl/fl}$ or *Smarcb1*$^{fl/fl}$ MEFs. ChIP-seq experiments were performed on puromycin selected cells 96 hours after retroviral infection.

Supplementary Figure 6. Related to Figures 1-7: Models of signal-dependent enhancer selection by AP-1 TFs and SWI/SNF

Prior to Ras/MAPK activation, the constitutively expressed AP-1 TF JunD and putative fibroblast LDTFs Tead and Ets family TFs cannot bind stably to the enhancer because it is bound to a histone octamer. Activation of the Ras/MAPK signal transduction cascade by growth factors or other extracellular stimuli induces high levels of transcription of the ERG AP-1 TFs (Fos, Fosb, Fosl1/2, Jun, Junb), which, unlike JunD, can interact with SWI/SNF. (**a**) Collaborative competition model: In this scenario, AP-1 and LDTFs compete directly for binding to the enhancer sequence with the histone octamer. Prior to induction of high levels of AP-1, the LDTFs alone are not sufficient to outcompete the histone octamer, and are not likely to be able to bind stably to their motifs on the nucleosome. After eviction of the histone octamer by AP-1 and LDTFs, SWI/SNF is recruited to the enhancer by AP-1 and it further remodels flanking nucleosomes to stably establish accessible chromatin. (**b**) Hierarchical/pioneer factor model: In this scenario, AP-1 TFs bind to the enhancer first and recruit the SWI/SNF complex to remodel nucleosomes, enabling other LDTFs to subsequently bind. (**c**) LDTF priming model: In this scenario, LDTFs can bind to enhancers before AP-1 TFs are activated, but they cannot bind stably and are not sufficient to establish accessible chromatin. However, the binding of these LDTFs is required to make AP-1 motifs on nucleosomes accessible for AP-1 TF binding. AP-1 TFs then function to recruit SWI/SNF to these sites to remodel nucleosomes and establish accessible chromatin.